Estimating frequency stability margin for flexible under-frequency relay operation

Rudez Urban[a,*], Sodin Denis[b], Mihalic Rafael[a]

[a] *University of Ljubljana, Faculty of Electrical Engineering, Trzaska 25, 1000 Ljubljana, Slovenia* [b] *COMSENSUS, Brezje pri Dobu 8a, 1233 Dob, Slovenia*

Abstract

SmartGrid solutions are often misinterpreted as complex approaches requiring large amounts of (online) data and computational power for delivering high-quality results. With today's technology, this is surely the most obvious and technically achievable approach for dealing with complex problems. However, by taking this road in the power system field, providing the required high-level reliability becomes a challenging task. Therefore, a thorough consideration of whether increased complexity justifies the gains is surely warranted, especially when it comes to power system protection, where the applied procedures are all about transparency, simplicity and robustness – which is often in contrast to the above interpretation of SmartGrids. Therefore, the motivation of the presented research was to design an effective SmartGrid solution for avoiding power system frequency instability, appropriate for real-life application. Under-frequency load-shedding protection is the subject of many research activities that often result in complex and, consequently, unfeasible suggestions. In contrast, this paper presents an effective *RoCoF*-based upgrade to the conventional approach, eliminating its most important shortcoming: inflexibility. By estimating frequency stability margin in real time, shedding decisions remain local, whereas the overall efficiency of this system protection scheme is brought to the level of the most sophisticated solutions available in the literature.

Keywords

Power system dynamics, Power system protection, Smart grids, Power system measurements, Power system stability

List of abbreviations

COI	centre of Inertia
ENTSO-E	European network of transmission system operators for electricity
EPS	electrical power system
$f(t)$	electrical power system frequency [Hz]
f_{LIM}	frequency stability limit [Hz]
$f_{thr,i}$	*i*th sequential frequency threshold [Hz]
H	inertia constant [s]
$M(t)$	frequency stability margin [s]
$M_{thr,i}$	ith sequential frequency stability margin threshold [s]
PMU	phasor measurement unit
$P_{thr,i}$	shedding amount designated to the ith sequential frequency threshold [%]
$RoCoF(t)$	Rate of change of frequency [Hz/s]
RTDS	real-time digital simulator
SIPS	system integrity protection scheme
t	time [s]
T_{dF}	timer setting for frequency threshold violation [s]
T_{dMF}	timer setting for frequency stability margin threshold violation (fast) [s]
T_{dMS}	timer setting for frequency stability margin threshold violation (slow) [s]
T_{RF}	sliding window width for RoCoF filtering (fast) [s]
T_{RS}	sliding window width for RoCoF filtering (slow) [s]
UFLS	under-frequency load shedding
WAMS	wide-area monitoring system

1. Introduction

One of the main reasons for the extreme level of efficiency of modern electrical power systems (EPSs) lies in how emerging technologies are treated and implemented by power system utilities. A very conventional approach in the process of harvesting capabilities of new technologies often seems rather unnecessary and difficult to comprehend. However, throughout the years, EPSs have become the leading infrastructure in supporting modern society's existence and so indispensable in a variety of ways. They became the most notable representatives of the so-called critical infrastructure. Many areas of human activities are so dependent on an EPS's operation that conditions emerging from blackouts are often unimaginable (social unrest, food shortage, increased crime rate, etc.) [1]. For this reason, system integrity protection schemes (SIPS) were introduced to prevent system operating conditions leading to blackouts. Major system imbalances between active power generation and consumption are being dealt with by under-frequency load-shedding (UFLS) protection. The conventional UFLS setting ([2,3]) appeared satisfactory up until the last decade or so when the penetration level of intermittent converter-based generation units began to seriously interfere with EPS inertia. Consequently, EPS frequency responses to active power imbalances became more turbulent in terms of the increased Rate of Change of Frequency (*RoCoF*). This led to the need for the under-frequency protection devices to enable *RoCoF* calculation in real time. In order for the measured *RoCoF* to be highly accurate, a time window of at least 100 ms is required. Nevertheless, *RoCoF* obtained from a shorter time window can also give some rough indications of a potentially dangerous situation, however, one should handle its value with care. Despite the above, many algorithms that extract appropriate information from *RoCoF* are still under research.

Several approaches to using *RoCoF* for UFLS purposes can be found in the existing literature. The large majority of them rely on knowing the relation between the active power imbalance and *RoCoF* that corresponds to a single synchronous machine (e.g. [4]) – the swing equation [5]. Substituting the entire set of individual machines with an equivalent generator enables one to study the average EPS frequency response, usually referred to as the Center of Inertia (COI) [6]. However, such solutions have a tendency to increase the UFLS complexity with the involvement of wide-area communication and the estimation of (mostly unknown) EPS

inertia (such as [7–10]). In contrast to such suggestions, this paper formulates the technology of a *RoCoF*-based modification of conventional UFLS based entirely on locally-obtained measurements and the estimated value of the frequency stability margin, which helps to recognize the need for immediate UFLS activation. A brief preliminary and elementary explanation of the concept in terms of basic principles and initial observations can be found in [11], whereas this paper presents its extensive in-depth formulation and analysis. The modification introduces an additional shedding criterion which significantly increases the scheme's flexibility to changes in operating conditions. This criterion is developed from an innovative representation of operating conditions in a newly-defined plane, which differs from commonly used frequency versus *RoCoF* planes ([12,13]). Apart from this, several further possibilities for user-defined UFLS settings emerge from the proposal that might open up a wide array of additional variations in the future. The concept was proven in [14] with real-time digital simulator in a hardware-in-the-loop setup that also served for improving *RoCoF* filtering technique and supporting the applicability of the approach.

2. Current status of conventional UFLS

2.1. Basic facts

Currently, most of UFLS schemes used in practice are of the conventional type, encompassing several stages ([5, 15,16]). The setting of each stage includes its size (amount of disconnected consumption/load, in practice achieved by tripping appropriate feeders) and the corresponding frequency threshold at which it is being activated. However, load feeders (assigned to an individual stage) are subjected to different power flows depending on different factors, such as the season within a year, day in a week, time of day, etc. In addition, in EPSs with a high penetration of distributed energy sources, power flow can be even more diverse due to the volatile character of such generation units. Therefore, a certain load feeder does not always represent the same share of the entire EPS loading, whereas a large group of feeders inter-balances those divergences introduced by individual feeders relatively well. This is the reason why individual stages are (as much as possible) uniformly dispersed among the loads in the system. This is not something that we were dealing with in this paper, since approaches to setting UFLS schemes of this type vary from one EPS to another, depending on the operator's experience and requirements. They differ in:

- the number of shedding stages (denoted by n),
- the frequency thresholds setting ($f_{thr,i}$ where i = 1,…, n),
- the shedding size (amount) associated with each stage ($P_{thr,i}$ where I = 1,…, n) and
- the maximum sum of all disconnections ($P_{tot} = \sum P_{thr,i}$).

The electrical voltage frequency (the only UFLS triggering criterion) is being measured at the under-frequency relay location itself (i.e. at the individual load feeder) or, in some cases, in a single place within the substation and then communicated to relays within the substation. When it comes to the research community, both solutions fall into the category of *local measurements*. UFLS schemes harvesting from local measurements are much more favorable in practical applications compared to other solutions, as the absence of the need for wide-area communication networks significantly increases the scheme's efficiency and reliability.

2.2. Shortcomings

In terms of quantity, the conventional UFLS approach actually has very few shortcomings. However, that does not mean that their consequences are negligible. Conventional UFLS complies well with words like transparency, simplicity and robustness. On the other hand, among those few deficiencies, the *non-adaptive* character to a variety of possible situations they might encounter should certainly be highlighted. This mostly relates to unacceptable frequency overshoots that result from the frequency threshold violation being the only UFLS triggering criterion. By increasing the number of stages n and, therefore, decreasing *all* the associated shedding amounts per stage $P_{thr,i}$, conventional UFLS gains more and more adaptive capabilities. On the other hand, introducing different distribution patterns of P_{tot} among stages [17] results only in certain stages decreasing at the expense of others. The mere presence of stages with large $P_{thr,i}$ indicates potential overshoots, as they are triggered regardless of *RoCoF*.

By definition, the objective of UFLS is to "prevent a further frequency drop" [18] or, in other words, "restore the balance" [19] between the generated and consumed active power in the EPS in due time, i.e. before the frequency drops below the frequency stability limit. Therefore, it seems reasonable to clearly distinguish between frequency control and UFLS objectives: *i*) the task of an automated UFLS is to stop the frequency decline and is followed by *ii*) frequency control that brings the frequency back to a nominal value.

Let us consider using a validated real EPS model [20] for performing dynamic simulations of frequency stabilization after the model is stressed by a wide array of active power imbalance amounts. In each situation, different settings of conventional UFLS are applied in terms of the number of shedding stages n. The total sum of individual stage amounts is kept constant (P_{tot} = 50% of the power system loading) and the corresponding frequency thresholds are linearly distributed between 49.0 Hz and 48.0 Hz in all cases (see Fig. 1).

The results of the analysis are presented in Fig. 2. In the upper graph, the attained load disconnection amounts are presented with respect to different simulation cases (39 in total), each of them providing different active power stress imposed to the model (sorted in an ascending manner along the abscise axis). The results corresponding to a four-stage setting (n = 4) are depicted with the thick gray curve, whereas results of the ten-stage setting (n = 10) are represented with the thick black curve. The rest of the curves (thinner and all of the same gray color) represent the remaining schemes encompassing settings between five and nine stages (n = 5, 6, 7, 8 and 9, respectively). It is obvious that by increasing the number of stages n, the resulting curve in the upper graph gets closer and closer to a linear dependence on the seriousness of the disturbance. In theory, increasing the number of stages towards infinity would yield a perfect adaptability of such a scheme to any situation. In practice however, a number larger than ten stages is very rare.

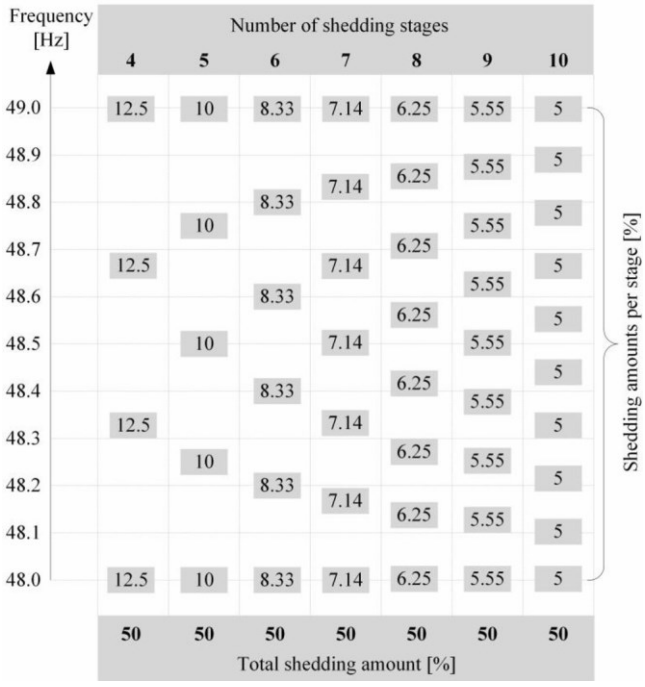

Fig. 1. The schematic representation of tested conventional UFLS settings.

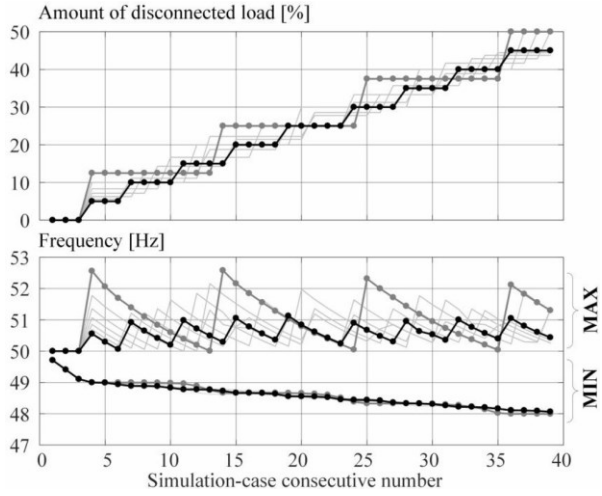

Fig. 2. Conventional UFLS testing results, according to Fig. 1 settings.

As long as conventional UFLS is in question, predefined blocks of load feeders are disconnected within an individual stage. The smaller the number of stages, the larger the blocks and, consequently, the larger the discrete steps in the upper graph of Fig. 2. These discontinuous changes coincide with situations when frequency violates a frequency threshold with a very small *RoCoF* of a negative value. For an improved frequency response, either a smaller portion of a corresponding block would have to be disconnected by UFLS or the situation should be left for the frequency control mechanism to handle. Instead, the entire block is tripped which results in overshedding and, in terms of frequency, a frequency overshoot. This is confirmed by additionally analyzing the lower graph in Fig. 2, which includes two sets of information: minimum (MIN) and maximum (MAX) frequency value recorded during each simulated transient. The curve color and thickness properties are the same as in the upper graph of the same figure.

Increasing the number of stages does not affect the scheme's ability to prevent frequency drops in any way. This is expected, as UFLS plays the role of under-frequency protection and has proven satisfactory throughout many years of operation (high *RoCoF* conditions as well). On the other hand, it affects recorded overshoots significantly; in case of a four-stage setting, the largest recorded overshoots reach as high as 52.5 Hz, whereas in the case of a ten-stage setting, they are kept below 51.0 Hz. So actually, in many situations, instead of providing an appropriate solution to an under-frequency problem, it merely creates an over-frequency problem due to the lack of flexibility of conventional UFLS to adjust the scale of its intervention.

Any UFLS re-setting in terms of changing the number of stages *n* requires a complex and lengthy procedure to be performed by the system operator. Therefore, finding an alternative solution for soft-tuning the UFLS intervention at low *RoCoF* conditions is the motivation of this paper. In continuation, a much simpler and easy-to-implement alternative for achieving similar effects on EPS frequency response is presented. It requires setting an *additional criterion* for the activation of each existing load-shedding stage.

3. Introduction to the *RoCoF*-based criterion

3.1. Background

The idea for the presented *RoCoF*-based criterion arose from the existing set of *predictive UFLS* suggestions. The feasibility of the initial attempts of applying the second time derivative of the COI frequency [21] for short-term prediction of the frequency response was indeed questionable in terms of practical applications. However, they inspired several publications that followed, each of them eliminating a few questionable elements. As a result, a WAMS-based predictive UFLS was suggested in [22], taking advantage of the EPS frequency only, obtained from a couple of PMU (Phasor Measurement Unit) measurements in the EPS. The quality of the results proved to be high and it was thus considered as a target performance. Nevertheless, the motivation remained for bringing shedding decisions back down to the local level with the help of prediction strategies without the need for any centralization.

3.2. Definition

Looking at Section 2.2, it becomes obvious that the existing UFLS schemes lack the capability of recognizing conditions when shedding could be delayed without jeopardizing the EPS frequency stability. This is why we believe that an additional shedding criterion is required for each stage which would prevent overshedding when there is still some leeway left before the EPS frequency instability occurs (in this paper defined by a violation of the frequency limit f_{LIM}, usually 47.5 Hz, but it can be arbitrarily selected).

To this end, *RoCoF*(t) is applied alongside frequency $f(t)$ with the aim of predicting/estimating the *frequency stability margin* $M(t)$, which can be expressed as the remaining time before f_{LIM} is violated. Both *RoCoF*(t) and $f(t)$ are considered time-dependent variables, calculated internally in all processor-based under-frequency relays. The $M(t)$ calculation can easily be performed in real time within the relay itself as it follows a very straightforward equation, whose structure is represented graphically by Fig. 3:

$$M(t) = \frac{f_{LIM} - f(t)}{RoCoF(t)} \tag{1}$$

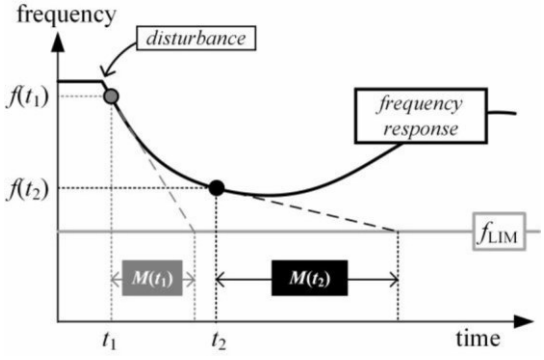

Fig. 3. Graphical representation of the stability margin calculation $M(t)$.

Next, the frequency $f(t)$ versus $M(t)$ diagram is introduced – see Fig. 4. Fig. 4a depicts the operation point trajectories for occurrences of several active power deficit conditions when no load shedding takes place. In steady-state conditions, frequency $f(t)$ = 50 Hz and *RoCoF*(t) = 0 Hz/s, i.e. the $M(t)$ is calculated as infinite. So prior to disturbance, the operation point is located in the upper right-hand side of the $f(t)$ versus $M(t)$ diagram. After the disturbance, causing an active power imbalance, the operating point relocates and initially follows the trajectory towards the bottom left part of the diagram. The trajectories, corresponding to cases when f_{LIM} is eventually violated, converge towards the diagram origin, whereas in the rest of the cases (when frequency stability is maintained), the trajectory is sooner or later re-directed back towards the right-hand side of the diagram, corresponding to large values of $M(t)$ as an indication of small *RoCoF*. We are able to use this distinction between potentially stable and unstable cases effectively by setting the second shedding criterion, described in Section 3.3.

For clearer presentation, Fig. 4b depicts the corresponding frequency versus time curves (time-domain simulations) and three snapshots at arbitrarily-selected moments in time. They are denoted by dots at simulation points t = 3.85 s, t = 5.85 s and t = 7.85 s.

3.3. Additional shedding criterion

In a frequency $f(t)$ versus $M(t)$ diagram (e.g. Fig. 4a), shedding criteria of conventional UFLS can be represented by means of horizontal lines, each of them corresponding to an individual shedding stage (see an exemplary 3-stage UFLS in Fig. 5a). Such characteristics are employed in each under-frequency relay, depending on the load block into which an individual load feeder is assigned. It is clear from Fig. 5a that in most cases, the first shedding stage would be activated at frequency $f(t) = f_{thr,1}$ regardless of the underlying circumstances. This seems unnecessary as examining the lower graph of Fig. 4b reveals that even if the first stage was blocked, the frequency control alone is fully capable of stabilizing the frequency in three more cases. Not only would this keep several loads supplied, but it would also avoid an unnecessary overshoot.

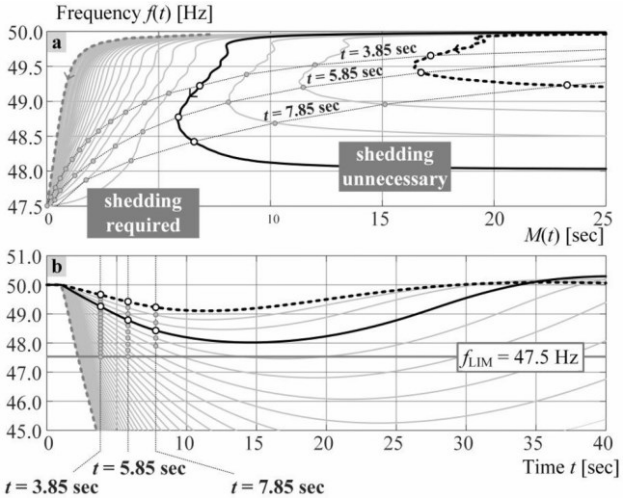

Fig. 4. EPS frequency response; frequency $f(t)$ versus $M(t)$ diagram (a), frequency $f(t)$ versus time t (b).

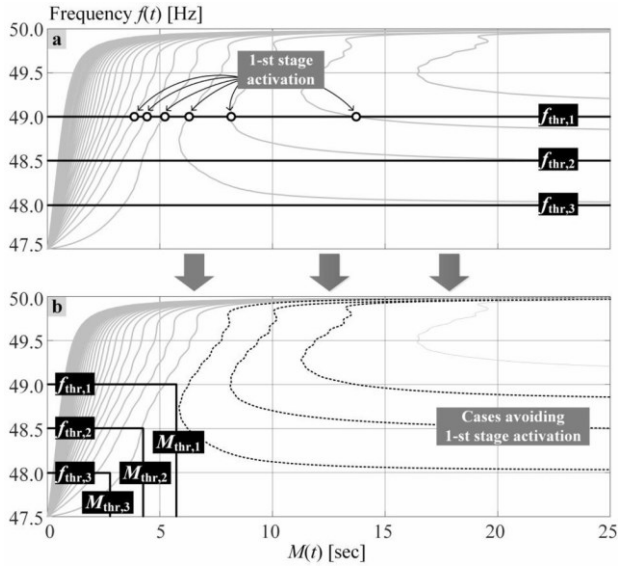

Fig. 5. Traditional (a) and suggested (b) setting of UFLS after introducing the additional shedding condition $M_{thr,i}$.

As already explained, the task of UFLS is not to bring the frequency back to the nominal value, but to bring *RoCoF*(*t*) back to the value of zero by regaining an active power balance in an EPS. Once this is achieved, bringing the frequency back within the desired limits according to grid code depends on the frequency control. Distinguishing between both actions can be achieved by applying the described concept using $M(t)$. A modification of the existing UFLS by introducing an additional shedding criterion $M_{thr,i}$ in each shedding stage is suggested, according to Fig. 5b. Conceptually, for large values of $M(t)$ (which predicts the violation of f_{LIM} far in the future), the activation of individual shedding stages is put on stand-by despite the corresponding frequency threshold being violated. Since large values of $M(t)$ indicate a small RoCoF and, therefore, an almost stable frequency, this is considered a frequency control problem. On the other hand, small values of $M(t)$ indicate the immediate need for UFLS activation. We suggest that each UFLS stage (e. g. stage i) ought to be modified from setting frequency thresholds $f_{thr,i}$ alone towards setting a pair of values $f_{thr,i}$ and $M_{thr,i}$. In this way, the UFLS performance becomes superior compared to simply setting fixed time delays to 81 relays. The new criterion indirectly incorporates a *varying* time delay to each UFLS stage that depends on the actual system conditions, which of course vary in time.

3.4. Possibility of introducing substages

An important contribution of the presented approach is the introduced flexibility of UFLS, which significantly exceeds that of the conventional philosophy. One can intentionally introduce substages to each UFLS stage by setting different M_{thr} values to relays despite having identical f_{thr} (see Fig. 6). Substages become relevant when frequency decays are moderate, otherwise they remain irrelevant (e.g. during extremely fast decays). In this way, a soft-tuning of the disconnection procedure is achieved, which always appears in form of a more favorable frequency response. To a certain extent, substages seemingly appear even as an inherent by-product of the methodology since *RoCoF* is more oscillatory in nature compared to the frequency itself [23]. In this way, when/if inter-generator oscillations appear after the disturbance, some under-frequency relays (corresponding to the same frequency threshold) are triggered faster than others, depending on their location in the EPS. *RoCoF*(*t*) being prone to location-dependent oscillations is, therefore, seen as an advantage opposed to most of other approaches in the literature. In this paper a test network was intentionally selected such that the oscillations were minor in order to stress the impact of a mere presence of M_{thr} thresholds.

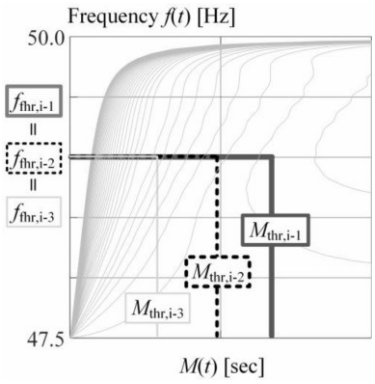

Fig. 6. Intentionally introducing three substages to a selected UFLS stage *i* with identical frequency thresholds ($f_{thr,i-1} = f_{thr,i-2} = f_{thr,i-3}$), but different frequency margin thresholds ($M_{thr,i-1} \neq M_{thr,i-2} \neq M_{thr,i-3}$).

3.5. Sensitivity to RoCoF calculation requirements

The application of *RoCoF* for UFLS protection often raises several doubts. The argument is mostly whether or not there is enough time available to provide an adequately precise *RoCoF* measurement in extreme active power imbalance conditions. To this end, we analyzed the EPS frequency response following two different events: *i*) a small power imbalance causing an initial *RoCoF* of − 0.5 Hz/s and *ii*) a large power disturbance resulting in an extreme *RoCoF* of − 5 Hz/s.

We assumed the availability of raw frequency and *RoCoF* measurements at a 50 Hz reporting rate (time resolution of 20 ms). Next, we applied a sliding window with an adjustable width (from 50 ms to 500 ms) to *RoCoF* measurements. We further averaged all measurements within the sliding window (creating a sliding average window), representing a simple yet effective way of cancelling input data noise. Finally, we observed the results in the frequency $f(t)$ versus $M(t)$ diagram, presented in Fig. 7.

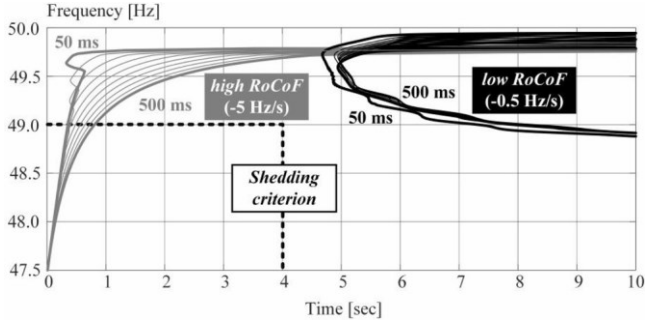

Fig. 7. Sensitivity to RoCoF sliding window width calculation.

When the frequency's initial drop is at a rate of − 0.5 Hz/s (solid black curves in Fig. 7), the *RoCoF* calculation appears almost insensitive to variations in the sliding window width. This was expected due to the slow frequency variations. Surprisingly, the sensitivity to window width is not that critical even when the frequency drop is at a rate of − 5 Hz/s (solid gray curve in Fig. 7), as long as we consider UFLS activation below 49.0 Hz. Nevertheless, in order to be cautious enough with respect to extreme *RoCoF* situations, we suggest two independent parallel *RoCoF* calculations, the first one based on a narrow time window (T_{RF}) and the second one based on a wider time window (T_{RS}). We assume that either one of the *RoCoF* calculations should be able to initiate relay tripping (see logical OR gate in Fig. 8). The philosophy behind it is that once frequency violates one of the thresholds and at least one of both *RoCoF* calculations indicate the need for shedding, it is better to perform disconnections preventively as opposed to risking a total EPS blackout. By doing so, we achieve that, in extreme conditions, the relay trips due to the violation of the f_{thr} criterion alone.

3.6. A logical block diagram and the procedure for setting an additional shedding criterion

In order to show that the realization of the suggested modification is feasible with the existing hardware (i.e. protection relay), a logical block diagram is provided containing all vital elements – see Fig. 8. Both raw input variables, $f(t)$ and $RoCoF(t)$, are first processed by a sliding average window element. As described in Section 3.5, $RoCoF(t)$ is handled by two separate sliding window elements, being different in the order of the selected window width. The first one (index "S") represents a slow and more accurate *RoCoF* calculation, whereas the second (index "F") represents a faster and less accurate *RoCoF* calculation.

In the continuation, only negative *RoCoF* values are of interest, which we carried out by means of a limitation block. Next, (1) is applied to obtain the frequency stability margins $M_F(t)$ and $M_S(t)$. We performed the comparison of frequency as well as time margin to predefined threshold values with two consecutive elements, the summation and hysteresis block. They provide the binary value of 1 when an individual threshold is violated and 0 when it is not. Every time any of those binary values change from 0 to 1, they trigger the timer elements, and once the duration of each threshold violation lasts long enough (according to pre-set durations T_{dF}, T_{dMS} and T_{dMF}), variables f_V, M_{VS} and M_{VF} are set to 1, respectively. Both frequency stability margin (either M_{VS} or M_{VF}, for explanation see Section 3.5) and frequency are required to violate their respective thresholds simultaneously in order to generate the output trip signal.

It is also important to provide some guidelines on how to set the thresholds corresponding to an additional shedding criterion $M_{thr,i}$. First, we have to clearly explain what could theoretically be the worst possible impact of doing this inappropriately:

- by setting $M_{thr,i}$ thresholds to an extremely large value, we basically obtain a conventional UFLS setting. Most of the time, the calculated $M(t)$ would be less that the threshold and, therefore, one out of two tripping criteria would always be fulfilled, which eventually means we are dealing with a conventional UFLS,
- by setting $M_{thr,i}$ thresholds to a very low value, we basically pause a corresponding UFLS stage until the frequency reaches the very lowest acceptable limit of f_{LIM}. This means that the corresponding UFLS step is still activated, but at the very last moment before reaching f_{LIM}. This presents the potential for having a positive impact in case governors alone suffice for frequency stabilization, yet the negative impact would be delaying the shedding until the very last moment.

In this paper, we aimed to minimize the amount of disconnected consumers. This is why $M_{thr,i}$ thresholds are all set below 2 s (see Tables 1 and 2). These were obtained by following the steps depicted in Fig. 9. A prerequisite is to have a representative simulation model of the network alongside the governor controllers. Next, one is required to deactivate UFLS and set up an operating point with a minimal possible realistic amount of system inertia. After that, one is required to dynamically simulate the transition into island operation of the network by gradually increasing the amount of the active power deficit with a sufficiently low imbalance increment. The process stops once we detect a borderline case in which the frequency is successfully stabilized by governor control alone. By plotting this case in a frequency $f(t)$ versus $M(t)$ diagram, it should be straightforward to estimate an appropriate value of the first $M_{thr,1}$ thresholds. Finally, this step is activated and the increasing of the active power deficit may continue. The procedure is repeated until all UFLS steps are activated.

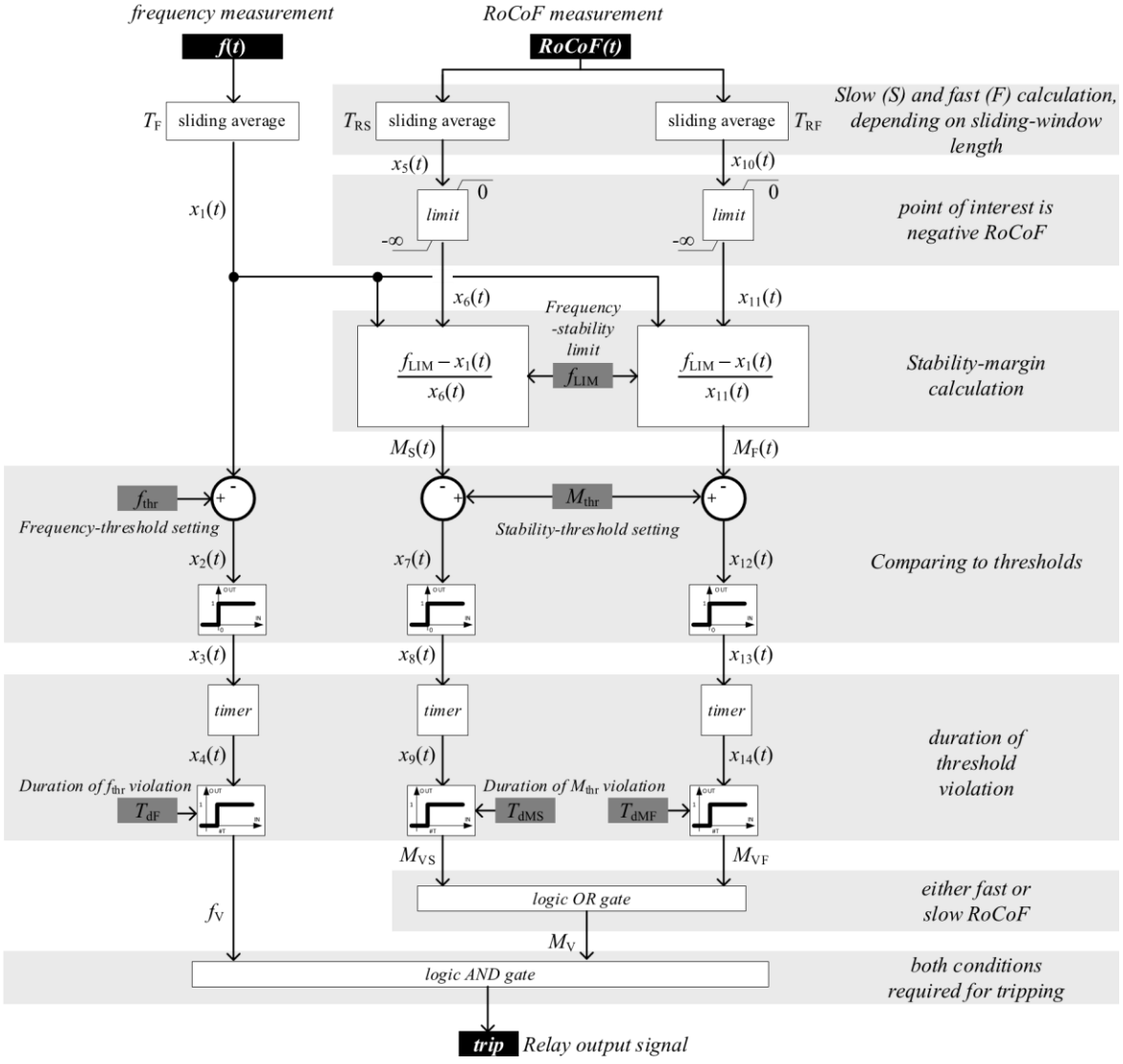

Fig. 8. Logical block diagram for the realization of the suggested modification in the under-frequency relay.

Table 1: Parameters of an applied 4-stage UFLS protection

Stage No.	f_{thr} [Hz]	M_{thr} [s] / decreased loading [%]
1.	49.0	2.0 / 10
2.	48.7	1.0 / 15
3.	48.4	0.8 / 15
4.	48.0	0.6 / 15

Table 2: Parameters of an applied 6-stage UFLS protection

Stage No.	f_{thr} [Hz]	M_{thr} [s] / decreased loading [%]
1.	49.0	2.0 / 10
2.	48.8	1.3 / 10
3.	48.6	1.1 / 10
4.	48.4	0.9 / 10
5.	48.2	0.7 / 10
6.	48.1	0.5 / 5

4. Case studies

4.1. Power system model

For a case study of the operation and efficiency of the presented approach, we used an existing EPS model. It encompasses a part of the 110 kV network of the Slovenian EPS. Since this model was successfully validated against PMU measurements before [20], the authors consider it appropriate. It consists of twelve hydro units with synchronous generators having an equivalent inertia constant of 6 s (exciter, governor) and nine substations. We modeled each out of the nine substations as having ten load feeders, whereas only half of them were included in the UFLS protection scheme. The rest of the Slovenian EPS was represented as a rigid power source with the appropriate short-circuit power, whose disconnection was considered as the main event causing active power imbalance conditions in the newly-formed island. The imbalance amount depends on pre-fault steady-state operating points of both machines and loads.

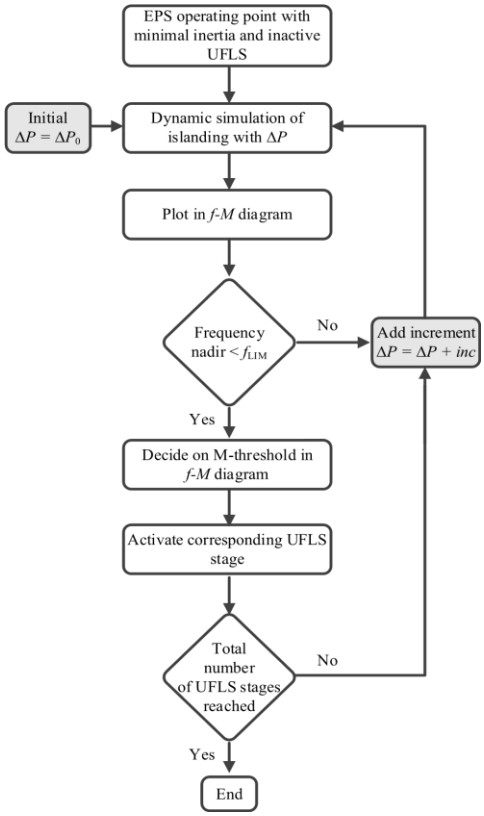

Fig 9. Flowchart guideline for setting $M_{thr,i}$ thresholds.

As for the UFLS setting, the presented modification was tested on both the existing 6-stage (in accordance with the ENTSO-E Policy 5 document [18]) and a 4-stage UFLS setting. For the reader's convenience, the specifics of both (i.e. frequency thresholds and corresponding amounts of shedding) were provided in Table 1. Apart from this, the selected frequency margin thresholds were listed in the same table as well. In order to avoid overcomplicating the paper, the testing is performed on a single added M_{thr} threshold per stage. With regard to EPS disturbances, a set of 60 simulation cases was used, encompassing possible active power imbalance amounts between 0% and 75%. The results are provided in Section 4.2. In addition, the same set of events was tested for the variated equivalent inertia constant of the island [24]. Results provided in Section 4.3 indicate that the presented methodology is quite independent of inertia. The parameters in the block diagram (Fig. 8) are identical in both cases: T_F = 20 ms, T_{RS} = 200 ms, T_{RF} = 20 ms, f_{LIM} = 47.5 Hz, T_{dF} = 20 ms, T_{dMS} = 100 ms, T_{dMF} = 100 ms.

4.2. Variation of the active power deficit

For a 4-stage UFLS, the overview of all 60 results is provided in Fig. 10. Results indicate that the imposed improvement to conventional UFLS successfully distinguishes between critical and non-critical situations, i.e. when UFLS activation is required promptly and when it is not. Indeed, any improvement can be

achieved only when having a non-zero frequency control volume available that is given more time to act. In this specific case, 10% of rated power of all involved machines was attributed to frequency control purposes.

It can be noticed that by adding the M_{thr} criterion to each of the four UFLS stages, we can avoid a frequency overshoot in practically all cases. To achieve that, the frequency is allowed to drop lower, but in a strictly controllable manner (never below f_{LIM}). If one does not feel comfortable letting the frequency drop so low, one can simply increase the value of f_{LIM} (e.g. to f_{LIM} = 48.0 Hz). Due to space limitation, these results are not included in this paper.

In 5 out of 60 cases, the reader might observe a slight increase in the overshoot compared to conventional UFLS. This is not the result of a foul UFLS concept, but a consequence of simplified logic in Fig. 8. Actually, recognizing such issues brings up an important topic that has to be discussed in order for the reader to fully understand the concept's pros and cons. The analysis showed that in those 5 cases discontinuous changes in $M(t)$, appearing after each shed, cause the resetting of duration timers in Fig. 8. As a consequence, the detected violation of a newly-adopted threshold is a bit postponed. During that time, an additional quantity of frequency control is mobilized. Since the shedding is inevitable, a slightly different power mismatch causes the frequency to increase slightly. It should be stated that this issue can be solved by having more sophisticated filtering of *RoCoF* (applying, e.g. a median filter instead of a sliding average). In practical applications, this would certainly be the case.

The analysis of two specific cases (case 14 with dashed curves and case 41 with solid curves) in the frequency versus time domain is presented in Fig. 11. Case 14 represents a less severe situation, where conventional triggering of the second UFLS stage too strongly reverses the power balance in favor of the generation. On the other hand, the newly-presented approach postpones the triggering of the first stage (activated slightly below 48.5 instead of at 49.0 Hz) and completely avoids the second one. When the frequency was passing frequency thresholds, real-time monitoring of $M(t)$ clearly indicated that there was still some leeway left to give the frequency control an opportunity to perform the task it was designed for. Since it was indeed successful in the stabilization of the frequency, a much smoother frequency recovery was achieved. If there was no more frequency control power available, the second stage still would have been activated later, creating no risk of endangering EPS security.

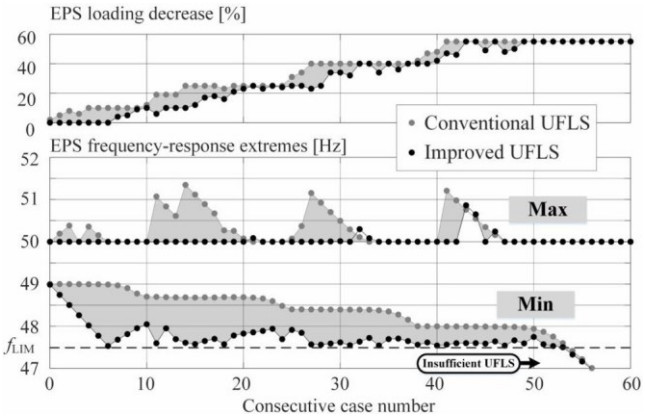

Fig. 10. Overview of the results gained by implementing the suggested changes to a 4-stage UFLS.

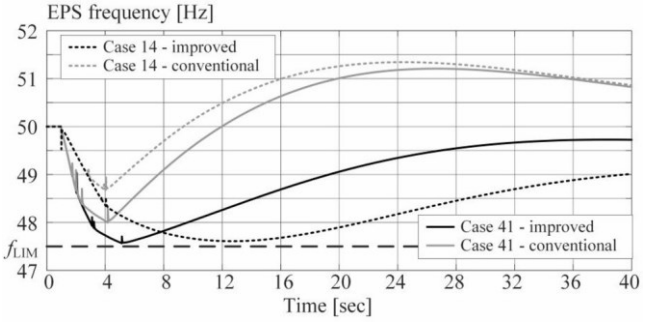

Fig. 11. EPS frequency response in two specific cases applying a 4-stage UFLS (Case 14 with dashed curves and Case 41 with solid curves).

A very similar situation takes place in Case 41. As long as the frequency drop is fast, both approaches ensure the consumers are disconnected by frequency threshold criteria. In this way, the first two stages are triggered at the same moment using both methodologies. Real-time monitoring of $M(t)$, on the other hand, delays the tripping of stage 3 and trips stage 4 only partially (due to the already discussed substages seemingly appearing as an inherent by-product of the concept).

For a 6-stage UFLS, an overview of all 60 results is presented in Fig. 12 in a similar manner as in Fig. 10. As expected, the overshoots obtained by applying conventional UFLS are lower compared to a 4- stage UFLS. Nevertheless, by introducing frequency stability margin monitoring, they are completely avoided in all simulated cases.

4.3. Variation of EPS inertia

According to current trends and predictions, we can expect a substantial decrease in EPS inertia in most countries worldwide. This means that the total rotational kinetic energy of synchronous machines left in operation will decrease. Not only that, due to the intermittency of renewable energy sources, we can expect the inertia to significantly variate in time. As a result, for the same amount of active power imbalance, one can expect more extreme values of *RoCoF*. This is why it is reasonable to test the efficiency of the presented methodology under changed inertia conditions.

Results in Section 4.2 were obtained by considering the equivalent EPS inertia of H = 6 s. In this section, results are additionally provided for both the decreased (H = 3 s) and increased (H = 9 s) inertia constant as well. On the other hand, for the entire duration of each simulation, inertia remained constant. The upper graph in Fig. 13 shows the detected frequency overshoots (among the same 60 simulated cases), sorted in a descending order, individually for each H value (see solid lines). Clearly, overshoots do not always appear using conventional UFLS, which is to acknowledge that sometimes conventional UFLS works properly. However, the lower the EPS inertia, the higher the number of cases with overshoots.

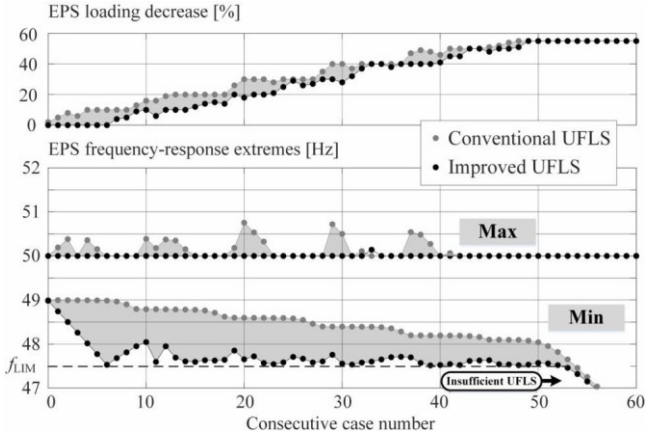

Fig. 12. Overview of the results obtained by implementing the suggested changes to a 6-stage UFLS.

Apart from a few outliers (dots whose colors correspond to individual EPS inertia values), the presented concept successfully eliminates frequency overshoot in the large majority of cases, independently of EPS inertia. As already elaborated in Section 4, those few outliers exist due to simplified programming and could be avoided with the implementation of an improved and more sophisticated *RoCoF* filtering method.

The middle and lower graphs in Fig. 13 show the difference between the conventional and improved UFLS approach: minimal detected frequency during the transient and the amount of disconnected consumers respectively. The results reveal that no significant changes arise with varied inertia. The average value of a minimum frequency change is around − 0.5 Hz (− 0.42 Hz, − 0.60 Hz and − 0.68 Hz, depending on EPS inertia), whereas the interval of case-to-case variations remains more or less unchanged. Similarly, no special changes appear in the amount of spared consumers either: on average, 5% of consumers remain in operation, regardless of EPS inertia and the severity of the power imbalance.

5. Conclusions

In this paper, a transparent and effective modification of a conventional UFLS relay setting is presented. It employs *RoCoF* for real-time frequency stability margin calculation, which is further monitored against the potential violation of newly-proposed frequency stability margin thresholds. The authors suggest implementing this new criterion in existing under-frequency relays alongside the already existing one. As a result, conventional UFLS gains the required flexibility with minimum intervention, regardless of the severity of the conditions.

The novel contributions of this paper are: *i*) the definition of an intuitively understandable time-dependent variable referred to as frequency stability margin $M(t)$, *ii*) the innovative representation of conditions in a frequency $f(t)$ versus frequency stability margin $M(t)$ plane, *iii*) introduction of a new UFLS triggering characteristic that represents a strong analogy to distance protection zones, *iv*) an explanation of further possible development by introducing UFLS substages, *v*) a sensitivity analysis of $M(t)$ calculation to different time requirements of a *RoCoF*- filtering phase, *vi*) a detailed logical block diagram that enables one to fully reproduce the results, *vii*) guidelines for setting the newly-defined thresholds, *viii*) a study of UFLS effectiveness under different power system inertia backgrounds and *ix*) a novel UFLS evaluation technique that will hopefully be adopted by other researchers as well.

The main features of the presented concepts are: *i*) the existing UFLS efficiency is not diminished by using *RoCoF* during a fast frequency decline (remains triggered by the existing frequency threshold violation), *ii*) increased flexibility to any given situation (active power imbalance, inertia), *iii*) UFLS operation remains based on local measurements and, therefore, highly robust, *iv*) locational oscillations of *RoCoF* during transients contribute to the flexibility. Further work on the subject will be concentrated on bringing the technology closer to real- life application, which involves improved *RoCoF* filtering and RTDS simulations.

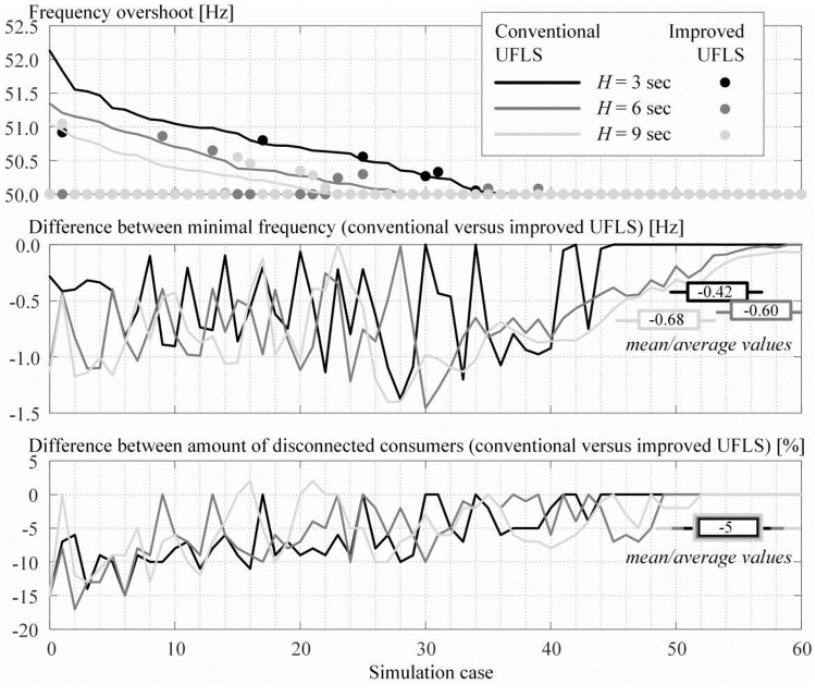

Fig. 13. Overview of the results obtained by implementing the suggested improvements to a 4-stage UFLS with a varied inertia.

Acknowledgments

This work was funded by the Slovenian Research Agency through the Electric Power Systems No. P2-0356 research program and the Resource management for low latency reliable communications in smart grids - LoLaG, J2-9232 project. The authors would like to thank the Slovenian Research Agency for the financial support. This work is subject to a pending International Patent Application No. PCT/EP2018/059048 filed on April 9, 2018.

References

[1] S. Matthewman, H. Byrd, Blackouts: a sociology of electrical power failure, Soc. Space (2014) 1–25.
[2] L. Sigrist, L. Rouco, F.M. Echavarren, A review of the state of the art of UFLS schemes for isolated power systems, Int. J. Electr. Power Energy Syst. 99 (2018) 525–539, https://doi.org/10.1016/j.ijepes.2018.01.052.
[3] N.M. Sapari, H. Mokhlis, J.A. Laghari, A.H.A. Bakar, M.R.M. Dahalan, Application of load shedding schemes for distribution network connected with distributed generation: a review, Renew. Sustain. Energy Rev. 82 (2018) 858–867, https://doi. org/10.1016/j.rser.2017.09.090.
[4] M.M. Elkateb, M.F. Dias, New proposed adaptive frequency load shedding scheme for cogeneration plants, in: Proceedings of the Fifth International Conference on Developments in Power Systems Protection, 1993, pp. 236–239.
[5] Y. Tofis, S. Timotheou, E. Kyriakides, Minimal load shedding using the swing equation, IEEE Trans. Power Syst. 32 (2017) 2466–2467, https://doi.org/10.1109/ TPWRS.2016.2614886.
[6] V.V. Terzija, Adaptive underfrequency load shedding based on the magnitude of the disturbance estimation, IEEE Trans. Power Syst. 21 (2006) 1260–1266, https:// doi.org/10.1109/TPWRS.2006.879315.
[7] P.M. Anderson, M. Mirheydar, An adaptive method for setting underfrequency load shedding relays, IEEE Trans. Power Syst. 7 (1992) 647–655, https://doi.org/ 10.1109/59.141770.
[8] S.-J. Huang, C.-C. Huang, An adaptive load shedding method with time-based design for isolated power systems, Int. J. Electr. Power Energy Syst. 22 (2000) 51–58, https://doi.org/10.1016/S0142-0615(99)00035-6.
[9] M.S. Pasand, H. Seyedi, New centralized adaptive under frequency load shedding algorithms, in: Proceedings of the Large Engineering Systems Conference on Power Engineering, 2007, pp. 44–48, https://doi.org/10.1109/LESCPE.2007.4437350.
[10] X. Lin, H. Weng, Q. Zou, P. Liu, The frequency closed-loop control strategy of islanded power systems, IEEE Trans. Power Syst. 23 (2008) 796–803, https://doi. org/10.1109/TPWRS.2008.920044.
[11] U. Rudez, R. Mihalic, RoCoF-based improvement of conventional under-frequency load shedding, in: Proceedings of the IEEE Milan Powertech, 2019, pp. 1–5, https://doi.org/10.1109/PTC.2019.8810438.
[12] V.N. Chuvychin, N.S. Gurov, S.S. Venkata, R.E. Brown, An adaptive approach to load shedding and spinning reserve control during underfrequency conditions, IEEE Trans. Power Syst. 11 (1996) 1805–1810, https://doi.org/10.1109/ 59.544646.
[13] L. Sigrist, I. Egido, L. Rouco, Principles of a centralized UFLS scheme for small isolated power systems, IEEE Trans. Power Syst. 28 (2013) 1779–1786, https:// doi.org/10.1109/TPWRS.2012.2227839.
[14] D. Sodin, R. Ilievska, A. Campa, M. Smolnikar, U. Rudez, Proving a concept of ˙ flexible under-frequency load shedding with hardware-in-the-loop testing, Energies 13 (2020) 3607, https://doi.org/10.3390/en13143607.
[15] B. Delfino, S. Massucco, A. Morini, P. Scalera, F. Silvestro, Implementation and comparison of different under frequency load-shedding schemes, Power Eng. Soc. Summer Meet. 1 (2001) 307–312, https://doi.org/10.1109/PESS.2001.970031.

[16] Y. Tofis, Y. Yiasemi, E. Kyriakides, A plug and play, approximation-based, selective load shedding mechanism for the future electrical grid, in: E. Luiijf, P. Hartel (Eds.), Critical Information Infrastructures Security, Springer International Publishing, 2013, pp. 74–83. http://link.springer.com/chapter/10.1007/978-3-319-03964-0_7 (Accessed September 9, 2014).
[17] J. Bogovic, U. Rudez, R. Mihalic, Probability-based approach for parametrisation of traditional underfrequency load-shedding schemes, IET Gener. Transm. Distrib. (2015), https://doi.org/10.1049/iet-gtd.2015.0533.
[18] RG CE OH – Policy 5: Emergency Operations V 3.1, (2017). https://docstore.entsoe .eu/Documents/Publications/SOC/Continental_Europe/oh/170926_Policy_5_ve r3_1_43_RGCE_Plenary_approved.pdf.
[19] ENTSO-E, Continental Europe Operation Handbook, Appendix 1: Load-Frequency Control and Performance, (n.d.). https://www.entsoe.eu/publications/system-o perations-reports/operation-handbook/Pages/default.aspx (Accessed February 23, 2015).
[20] D. Kopse, U. Rudez, R. Mihalic, Applying a wide-area measurement system to validate the dynamic model of a part of European power system, Electr. Power Syst. Res. 119 (2015) 1–10, https://doi.org/10.1016/j.epsr.2014.08.024.
[21] U. Rudez, R. Mihalic, A novel approach to underfrequency load shedding, Electr. Power Syst. Res. 81 (2011) 636–643, https://doi.org/10.1016/j.epsr.2010.10.020.
[22] U. Rudez, R. Mihalic, WAMS-based underfrequency load shedding with short-term frequency prediction, IEEE Trans. Power Deliv. 31 (2016) 1912–1920, https://doi. org/10.1109/TPWRD.2015.2503734.
[23] U. Rudez, R. Mihalic, Monitoring the first frequency derivative to improve adaptive underfrequency load-shedding schemes, IEEE Trans. Power Syst. 26 (2011) 839–846, https://doi.org/10.1109/TPWRS.2010.2059715.
[24] A. Fernandez-Guillam´ on, E. G´ omez-L´ azaro, E. Muljadi, ´ A. Molina-García, Power ´systems with high renewable energy sources: a review of inertia and frequency control strategies over time, Renew. Sustain. Energy Rev. 115 (2019), 109369, https://doi.org/10.1016/j.rser.2019.109369.